InGaAs/InP Single-Photon Avalanche Diode Detectors for Quantum Key Distribution

Gerald S Buller[1], Ryan E Warburton[1], Sara Pellegrini[1], Jo Shien Ng[2], John PR David[2], Lionel JJ Tan[2], Andrey B Krysa[2], and Sergio Cova[3]

[1] Heriot-Watt University, Riccarton, Edinburgh EH14 4AS, United Kingdom

[2]University of Sheffield, Sheffield S1 3JD, United Kingdom

[3]Politecnico di Milano, 20133 Milano, Italy

Abstract

The application of quantum key distribution has raised particular demands for single-photon detectors. The most promising candidate at the low-loss optical fibre communications windows has been the planar-geometry InGaAs/InP single-photon avalanche diode detector. These detectors have been modelled, fabricated, and characterized at 1.55μm wavelength. Their performance in terms of single-photon detection efficiency, dark count rate, timing jitter and afterpulsing behaviour are reported and compared with the best commercially available, linear multiplication diode APDs operated in Geiger-mode.

Detector structure

Linear multiplication avalanche photodiodes operating at the low-loss optical fibre windows of 1.3μm and 1.55μm wavelength generally use the separate absorption, grading and multiplication (SAGM) structure [1] [2]. The generic structure is shown in figure 1, and is designed so that photo-generated holes created in the narrow-gap InGaAs efficiently drift in a modest electric field into the wider-gap InP layer. The large valence band discontinuity between InGaAs and InP is smoothed by the use of a grading layer, in this case a mid-gap InGaAsP layer. The high probability of tunnelling in InGaAs at the high electric fields needed for multiplication means that it is necessary to use such a hetero-structure.

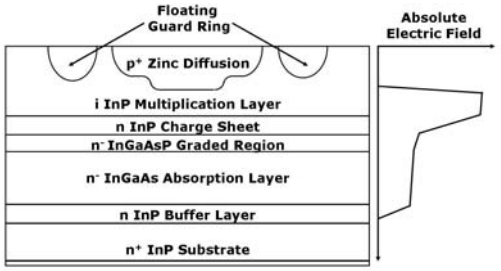

Figure 1: Cross-section of SPAD structure and absolute electric field (right)

These SPADs make use of this SAGM structure but have subtle enhancements specifically designed and modelled for use at electric fields above avalanche breakdown in Geiger-mode, and also at the low operating temperatures necessary to avoid a prohibitively high dark count rate.

Before the growth was performed, the devices were modelled with a commercial software package, ISE TCAD which was modified for these devices to ascertain the difference between the avalanche breakdown voltage (V_{bd}) and the punch-through voltage (V_{pt}); the lowest voltage at which the InGaAs absorbing layer is depleted. This is to ensure that the absorption region was fully depleted before the onset of avalanche breakdown, since V_{pt} does not change significantly with cooling in this temperature range, whereas the breakdown voltage reduces with decreasing temperature. Another consideration at the modelling stage was to ensure the electric field in InGaAs was kept suitably low to avoid tunnelling. In addition, another important issue was the avoidance of "edge-breakdown" where there is preferential avalanche breakdown at the edge of the p-n junction instead of in the centre of the device, coincident with optical access. For this reason a double diffusion of the p-type zinc dopant was chosen to form the p-n junction [2] since it exhibited a higher electric field along the central axis of the structure where the device was optically addressed. Floating guard-rings were also implemented to help reduce the electric field strength near the edges of the Zn diffusion fronts.

The structures were grown by metal organic metal vapour deposition (MOCVD), and used a 2.5μm thick layer of lightly n-type doped InGaAs for the absorber layer. The charge sheet used was a 300nm thick InP (n-type 6×10^{16} cm^{-3}) in order to reduce the electric field from the InP multiplication to the InGaAs absorption region. The multiplication region was ~ 1μm thick layer of nominally undoped InP, with a double diffusion of Zn to form the top p-type region. Part of the work was the investigation of the quaternary layer between the narrow-gap InGaAs and wide-gap InP [3]. Two separate structures were grown; SPAD 1Q, with a single quaternary of intermediate bandgap and SPAD 3Q with 3 separate quaternaries.

Photon-counting performance

The characterization set-up has been described in detail [3] [4]. All the optical measurements were conducted at λ ~ 1.55μm in gated mode operation, where the device was biased below V_{bd} by a dc bias, and then gated above breakdown for a short period around the expected photon arrival time [5]. In these measurements the gate duration was 100ns. At low temperatures, the effect of the quaternary layer on the single-photon detection efficiency (SPDE) and dark count rate (DCR) was noticeable. All the measurements were taken with a relative excess bias (V_{xs}) of 10%. It is clear that using more quaternary layers to smooth the valence band discontinuity results in a higher probability of the primary hole successfully entering the multiplication region. This is exhibited in the higher SPDE, which is especially notable at lower temperatures since the photogenerated holes have less thermal energy to overcome the barrier. This also explains the relatively lower DCR of SPAD 1Q at low temperatures. The best NEP was found to be ~ 1 x 10^{-16} $WHz^{-1/2}$ at 200 K as shown in figure 2.

An analysis of the jitter performance versus relative excess bias was performed for a 3Q structure with different device diameters of 10μm, 20μm and 40μm, as shown in figure 3. For these measurements, a pulsed laser of < 50 ps duration at FWHM was employed with the laser power reduced to permit a maximum count rate of no more than 10% of the clock frequency. This is necessary to avoid the effects of pulse pile-up [6] which could compromise the accuracy of the measurements.

The jitter results show a clear dependence on device diameter, due to the lateral spreading of the avalanche across the active area, observed previously in shallow-junction silicon SPADs [7].

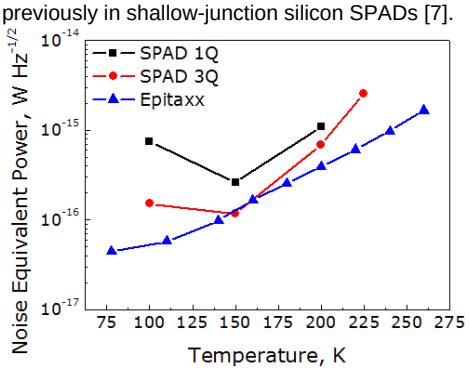

Figure 2: Noise equivalent power at λ ~ 1.55μm as a function of temperature for SPAD 1Q & 3Q compared to the best commercial APD (Epitaxx EPM239AA) operated in Geiger-mode.

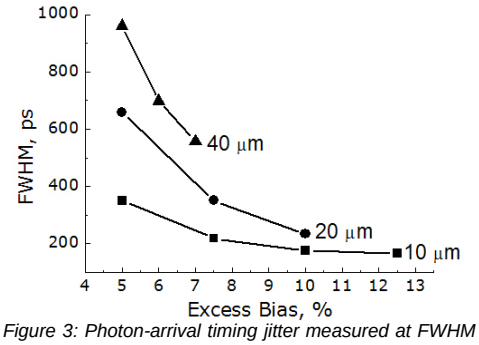

Figure 3: Photon-arrival timing jitter measured at FWHM of three SPAD 3Q devices of differing diameters. All measurements performed at a temperature of 175 K.

Afterpulsing

Whilst application requirements may be satisfied for single-photon counting at λ ~ 1.55μm with regards to SPDE, DCR and low jitter, InGaAs/InP SPADs are also affected by the deleterious effects of afterpulsing. The afterpulsing phenomenon is essentially a memory effect caused by the large amount of carriers that flow through the device during the avalanche process. Some of these carriers can become trapped in deep levels and are released after the avalanche event, and may contribute to the spurious counts in the measurement during the subsequent period. Since these SPADs are operated in gated mode, it is at least possible, in principle, to disable the SPAD for a sufficiently long length of time such that there is a negligible probability of a filled trap. If the device is enabled before all trap states are empty, it is possible that these carriers will be released and cause an unwanted count, or "afterpulse".

The afterpulsing probability was measured using the time-correlated carrier counting method [8]. The first gate in each period was kept at a fixed time and was coincident with the laser pulse containing multiple photons, so that there is a definite avalanche during the first gate, thus maintaining approximately the same amount of charge flowing through the detector in each period. The second gate was delayed by a variable time, Δt, and was scanned through the period. During the second gate, where no light is incident, only the "dark counts" are observed. For each value of Δt, the probability of a dark count was calculated on the basis of this measurement. After repeating this procedure for many values of Δt within one period, an afterpulsing probability distribution in time was obtained.

We performed this analysis on three separate samples; the best commercial-available linear multiplication APD operated in Geiger-mode (Epitaxx EPM239AA), an InGaAs/InP SPAD designed and grown within this project and a test structure which is essentially the same structure but without the InGaAs absorption region, nor the quaternary grading layer which will be referred to as "InP only". Each device was tested at varying temperatures to enable the data to be displayed in an Arrhenius plot so that the activation energy of the traps can be extracted. Using the afterpulsing probability at the longest delay, we find the point on the curve at which the afterpulsing probability is 10 times this value. This was repeated the other two structures and the values plotted in an Arrhenius plot shown in figure 5.

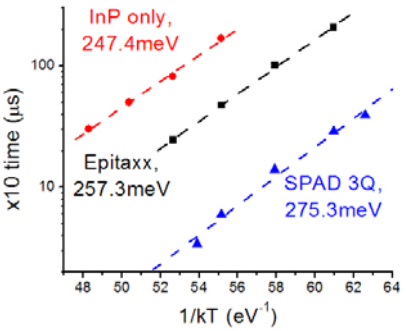

Figure 4: Arrhenius plot of times taken for the probability to reduce to a level of ten times the DCR for the three devices tested, with activation energies extracted and displayed.

The evidence in Figure 4 points to the InP being the location of the traps. This study was helpful to eliminate the other layers and, in particular, the interfaces between layers as the source of the traps.

Conclusions

We report a growth and fabrication programme for planar-geometry InGaAs/InP SPADs, and has produced detectors suitable for QKD in terms of timing jitter, SPDE and DCR. The afterpulsing is similar in behaviour to that found in the best commercially available InGaAs/InP APD operated above avalanche breakdown. By use of afterpulsing measurements at different operating temperatures, the activation energy of the trap states responsible for the afterpulsing effect was found to be ~250meV – similar to that found in a commercial APD of similar geometry and fabrication approach. Importantly, a test device with the InGaAs and InGaAsP layers removed, but the InP grown and fabricated under identical conditions, exhibits a similar activation energy to both complete structures. This is clear evidence that the InP layers are making the primary contribution to the afterpulsing phenomenon. Further experiments to reduce the effects of afterpulsing are continuing.

References

[1] J.C. Campbell *et al*., Electron. Lett., **20**, 5961984 (1984).
[2] Y. Liu *et al*., J. Lightwave Technol., **10**, p.182 (1992).
[3] S. Pellegrini *et al.*, IEEE J. Quantum Electron., **43**, p. 397 (2006).
[4] G.S. Buller *et al.* IET Optoelectronics, **1**, p.249 (2007)
[5] S. Cova *et al.*, Appl. Opt., **35**, p. 1956 (1996).
[6] W. Becker, *"Advanced Time Correlated Single Photon Techniques",* Springer (New York) (2005).
[7] A. Lacaita *et al.*, Appl. Phys. Lett., **67**, p. 2627 (1995)
[8] S. Cova *et al.*, IEEE Electron.Dev.Lett., **12**, p. 685 (1991)